RNI: DELENG/2005/15153
Regn No. DL (DS)-112/MP/2026-27-28
Rs.200

www.mycoordinates.org

Coordinates

ISSN 0973-2136
Volume XXII, Issue 06, June 2026
THE MONTHLY MAGAZINE ON POSITIONING, NAVIGATION AND BEYOND

AITL-WING-HITL

Telemanipulation of autonomous drones using Digital Twins of aerial traffic interfaced with WING

Development Communication in Sustainable Land Administration Practices in the Federal Capital territory Abuja

AITL-WING-HITL: Telemanipulation of autonomous drones using DT of aerial traffic interfaced with WING

The system is designed to intervene in scenarios, where an autonomous AI agent – the "new driver" – encounters conditions too complex or unorthodox for autonomy alone to handle. We present here the first part of the paper. The concluding part will be publsihed in July issue

Kaya Kuru
School of Engineering and Computing, University of Central Lancashire, Preston, PR1 2HE, UK
Software Engineering Department, Fenerbahce University, Ataşehir, İstanbul, 34758, Turkey

Sam Worthington
Worthington Sharpe Ltd., Unit 1.3s Halton Mill, Mill Ln, Halton, Lancaster LA26ND, UK [1]

Darren Ansell
School of Engineering and Computing, University of Central Lancashire, Preston, PR1 2HE, UK

John M. Pinder
School of Engineering and Computing, University of Central Lancashire, Preston, PR1 2HE, UK

Aadithya Sujit
School of Engineering and Computing, University of Central Lancashire, Preston, PR1 2HE, UK

Benjamin J. Watkinson
School of Engineering and Computing, University of Central Lancashire, Preston, PR1 2HE, UK

Keith Vinning
PilotAware Ltd., 19 John McGuire Crescent, Coventry, CV32Q, UK [2]

Lee Moore
PilotAware Ltd., 19 John McGuire Crescent, Coventry, CV32Q, UK [2]

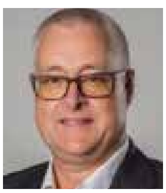

Chris Gilbert
PilotAware Ltd., 19 John McGuire Crescent, Coventry, CV32Q, UK [2]

David Jones
School of Engineering and Computing, University of Central Lancashire, Preston, PR1 2HE, UK

Claire Tinker-Mill
School of Engineering and Computing, University of Central Lancashire, Preston, PR1 2HE, UK

Abstract

"By touching an instrument placed in the southern gallery, a miniature Spanish cruiser anchored in the fountain lake on the lower floor, 90 ft away, was blown into the air. There was no connection between the transmitter and the vessel in the lake," reported The New York Times in 1898. Though perceived as magic by many at the time, Nikola Tesla had once again pushed the boundaries of technology, becoming the forefather of modern remotely controlled wireless drones. His invention – an early radio-controlled vessel operated via radio waves – was hailed as "the first of a race of robots, mechanical men which will do the laborious work of the human race," and marked a leap far ahead of its time. Since then, human–robot interaction and the telemanipulation of drones have advanced substantially, especially in tandem with the evolution of autonomy. In this context, a scalable, agent-based platform – termed AITL-WING-HITL – was developed for the telemanipulation of Autonomous Unmanned Aerial Vehicles (A-UAVs)

from the perspective of a human–multi-robot architecture, leveraging Digital Twins (DTs) of integrated aerial traffic. This system is designed to intervene in scenarios, where an autonomous AI agent – the "new driver" – encounters conditions too complex or unorthodox for autonomy alone to handle. The platform incorporates a patented, force-sensitive, precision control device known as the WING – an immersive tool tested with participants using measurable parameters to validate the system's effectiveness and identify areas for further improvement. The findings indicate that AITL (Autonomy-In-The-Loop) A-UAV agents and HITL (Human-In-The-Loop) Human Telemanipulator (HTM) agents can co-operate to achieve high-performance, synergistic task execution through a socio-cognitive interaction model embedded in the platform. By addressing current challenges and outlining directions for future exploration, this research not only provides an overview of the evolving landscape of drone telemanipulation but also serves as a roadmap for ongoing and future efforts in this critical field.

1. Introduction

"By touching an instrument placed in the southern gallery, a miniature Spanish cruiser anchored in the fountain lake on the lower floor, 90 ft away, was blown into the air. There was no connection between the transmitter and the vessel in the lake", reported The New York Times in 1898 [1]. Although many perceived it as magic, Nikola Tesla, once again pushing the boundaries of innovation, became the progenitor of modern-day remotely controlled wireless drones by inventing the first radio-controlled vessel using radio waves — an invention well ahead of its time [2]. This small radio-transmitting control box enabled Tesla to adjust the vessel's speed and direction by manipulating on-board mechanisms [3]. When a New York Times reporter described the invention as a device "that could carry dynamite as a weapon of war", Tesla responded: "You do not see there a wireless torpedo; you see there the first of a race of robots, mechanical men – a borrowed mind (the machine's own mind) – which will do the laborious work of the human race" [4]. His vision foreshadowed today's multi-agent autonomous robotic systems, capable of remote operation via distinct frequencies. Tesla's U.S. patent (US613809 A) referred to the invention as a "distant operator" – what we now call a teleoperator [3]. Since then, remote human–robot interaction and telemanipulation have evolved significantly alongside advances in autonomy. Many large-scale and complex tasks now require remote operation supplemented by extended human intelligence and experience. Drones are increasingly deployed by organisations and companies to execute various missions – such as logistics deliveries [5] – and operate in autonomous modes Beyond Visual Line of Sight (BVLOS) along preplanned routes. These missions must be conducted safely, avoiding collisions with other aerial vehicles within integrated Unmanned Aerial Vehicle (UAV) Traffic Management (UTM) and Air Traffic Management (ATM) systems, collectively referred to as the UTM+ATM framework.

In all future visions involving networks of fully autonomous self-driving ground [6] or aerial vehicles [7], some form of remote human intervention is anticipated. Specifically, roles such as "Human-on-the-Loop" (HOTL) and "Human-in-the-Loop" (HITL) for telemonitoring and telemanipulation are expected to foster a desirable level of trust in autonomous vehicles (AVs) as they operate within highly dynamic urban or aerial environments [8]. Ensuring the safe and cost-efficient routing of Autonomous UAVs (A-UAVs) within the integrated UTM+ATM system requires strategic human oversight: HOTL for fully autonomous UAVs (FA-UAVs) and HITL for semi-autonomous UAVs (SA-UAVs), enabling humans to monitor and intervene when necessary (Fig. 15) – particularly when the Artificial Intelligence (AI) agent, acting as the new "driver", encounters unorthodox scenarios beyond the scope of its autonomy. As automation continues to evolve, the nature of human–machine interaction has fundamentally shifted beyond the traditional Humans-Are-Better-At/Machines-Are-Better-At (HABA/MABA) paradigm, in which humans and machines are often seen as competitors [9]. Instead, the Human-Agent-Robot Teamwork (HART) frame-work emphasises collaborative augmentation, where humans and machines co-work by leveraging their complementary strengths to enable practical and profitable applications [10]. This paper examines co-work within this HART-centric framework from the perspective of two intelligent, self-reliant entities: humans equipped with extended intelligence and experience, and A-UAVs operating with a high degree of autonomy. These two entities are critically interdependent for the successful management of rare and complex challenges. Throughout the paper, the "human teleoperator" (i.e. master) and the "in-vehicle teleoperator" (i.e. slave) are referred to as the "Human Telemanipulator" (HTM), acting as the HITL agent, and the "A-UAV" (FA-UAVs and SA-UAVs, i.e. AITL agents), respectively.

Manipulating A-UAVs BVLOS will remain a central topic in the coming years, particularly as autonomous systems increasingly take on indispensable roles in real-world applications. In alignment with this trajectory, the University of Lancashire is actively developing bespoke A-UAVs and AITL systems 3 through various funded projects,4 aiming to tackle a wide range of complex operational tasks using A-UAVs. To support this mission, the University has partnered with PilotAware Ltd. and Worthington Sharpe Ltd. to ensure safe aerial operations, mitigating collision risks while enabling the execution of advanced aerial tasks. The core research question of this study is framed as follows: Can A-UAVs be effectively and efficiently manipulated through the collaborative operation of AITL and HITL agents? To explore this question, the following components were developed and integrated: (i) A Collision Management (CM) system, termed DACM (Drone Aware Collision Management) (Section 3.1.4), which creates Digital Twins (DTs) of aerial traffic through real-time communication with the decentralised PilotAware ATOM-GRID Network (Section 3.1.3); (ii) A patented, advanced force-sensitive control device, referred to as the WING, with 6DoF (Degree of Freedom) (Section 3.1.1), designed as an immersive precision-control interface for remotely operated vehicles (ROVs); (iii) A scalable agent-based platform – AITL-WING-HITL – that integrates these subsystems (Fig. 2) into a cohesive architecture, enabling HTMs to monitor and co-manipulate multiple A-UAVs within non-segregated aerial traffic environments, allowing human omnipresence.

While numerous novel robotic applications are anticipated, a range of emerging challenges must also be addressed — chief among them is ensuring that human–robot interaction remains safe, reliable, and effective [11]. One key question arises: Can the WING device facilitate effective interaction between HTMs and A-UAVs to accomplish tasks safely within the AITL-WING-HITL platform, especially given the potential limitations in human attention and perception when managing multiple A-UAVs simultaneously? To the best of our knowledge, this study represents the first comprehensive investigation into the use of a 6DoF advanced control device for manipulating multiple A-UAVs by a single HTM through digital replicas of aerial traffic, employing human–robot dialogue across several intervention modes (see Section 3.2.1). In addressing this research gap, the primary contributions of this paper are as follows:

(i) This research analyses the simultaneous manipulation of heterogeneous A-UAVs – autonomous aerial robots – by immersing HTMs within a newly integrated multi-agent architecture, termed AITL-WING-HITL.

(ii) The study explores the cooperative interaction between two intelligent entities – HTMs (HITL agents) and AITL AI agents – in performing complex tasks safely, accurately, and efficiently via various intervention modes (Fig. 15). This integration effectively bridges "the remote extension of human intelligence and expertise" with "vehicle autonomy".

The structure of the paper is outlined in Fig. 1 (see Table 1 for the abbreviations used in this paper).

2. Related works

A multitude of state-of-the-art studies have been conducted on the human telemanipulation of robots since the first teleoperator was built in the mid-1940s by Geortz [12]. Telerobotics, particularly bilateral robotic teleoperation activities between humans and robots, have generally been analysed based on the master and slave concept in which the slave side is mapped as "teleoperator" and the master side is mapped as "human operator" [8]. The supervisory role of human control in the remote manipulation of robots was first examined by Ferrell [13] in 1967. Most of the studies in the literature pay particular attention to HITL interactions, usually based on the semi-autonomous mode for human and single-machine hybrid activities to accomplish assigned tasks together, where semi-autonomous robotic systems are mainly designed with reliance on delay-tolerant human assistance [14]. The possibility of having multiple robots controlled by one operator (user) seems to be an additional crucial requirement in collaboration/cooperation [15]. Analysis of human–multirobot or human–multiagent cooperation and collaboration was immensely analysed in the 1990s as in [16–19], in particular, from the perspective of HITL decentralised systems, where the human needs to monitor the system all the time. The research of Nakauchi et al. [16] was the first in this direction in 1992. Laengle et al. [17] in 1997 had envisioned that "On one hand, robots have difficulties coping with unpredictable variations and uncertainties in their environment, which are normally no problem for humans. On the other hand, humans cannot always accomplish a task alone because of their limited force, slow execution speed, limited working area, limited execution time, and low precision. By combining the complementary capabilities of the robot with those of the human within a team, new perspectives for mastering complex systems could be opened". The seeds of HOTL robot manipulation were placed by Suzuki et al. [17] in 1995 while analysing the cooperation between the human operator and the decentralised multi-agent robotic system. The research emphasises several principles of HOTL as "(1) the human operator usually does not control each agent in the system,(2) all information of the system is not concentrated in the human operator, (3)

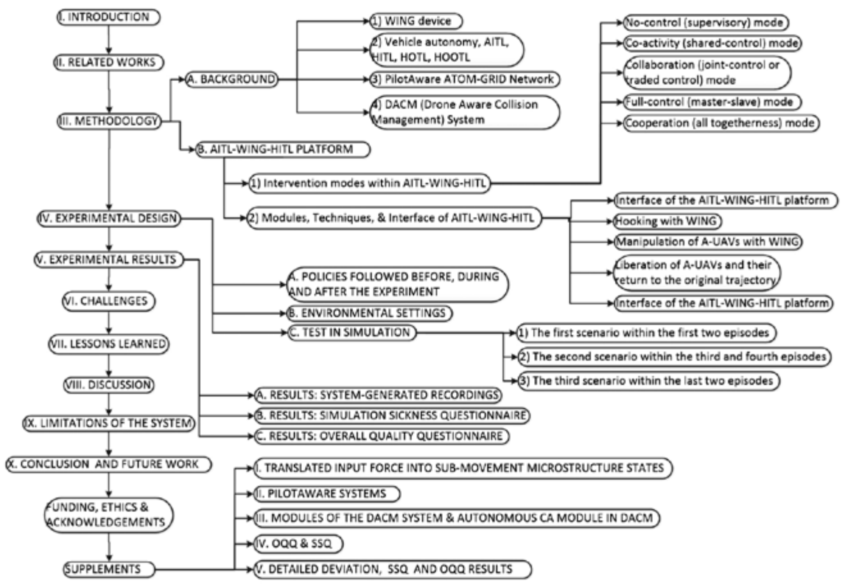

Fig. 1. Organisational structure of the paper.

Table 1
Definitions of abbreviations.

No	Abbreviation	Definitions
1	ADS-B	Automatic Dependent Surveillance-Broadcast
2	AI	Artificial Intelligence
3	A-UAV	Autonomous Unmanned Aerial Vehicle
4	AoE	Automation of Everything
5	AITL	Autonomy-In-The-Loop
6	ATM	Air Traffic Management
7	AV	Autonomous Vehicle
8	BVLOS	Beyond Visual Line of Sight
9	CA	Collision Avoidance
10	CAD	Computer-Aided Design
11	CPS	Cyber-Physical System
12	CM	Collision Management
13	CVP	Cartesian Virtual Point
14	DACM	Drone Aware Collision Management
15	DRONEII	Drone Industry Insights
16	DoF	Degree of Freedom
17	DT	Digital Twin
18	EC	Electronic Conspicuity
19	ECG	ElectroCardioGram
20	EEG	Electroencephalogram
21	ERDF	European Regional Development Fund
22	EASA	European Union Aviation Safety Agency
23	FAUAV	Fully A-UAV
24	FL	Federated Learning
25	FoSR	Flight of Safety Route
26	GUI	Graphical User Interface
27	HART	Human-Agent-Robot Teamwork
28	HABA	Humans-Are-Better-At
29	HITL	Human-In-The-Loop
30	HOTL	Human-On-The-Loop
31	HTM	Human Telemanipulator
32	ICAO	International Civil Aviation Organisation
33	IcRz	Imminent-collision-Risk zone
34	IoE	Internet of Everything
35	ICTZones	Imminent Collision Travel Zones
36	MABA	Machines-Are-Better-At
37	MAV	Manned Aerial Vehicles
38	mm-WAVE	Millimetre-Wave
39	MEDL	Minimum Expected Deviation Level
40	mMTC	Massive Machine-Type Communications
41	PC-UAV	Pilot-Controlled UAV
42	PcRz	Probable-collision-Risk zone
43	PCTZone	Probable Collision Travel Cone
44	RoI	Region of Interest
45	ROV	Remotely Operated Vehicles
46	QoE	Quality of Experience
47	QoS	Quality of Services
48	QoT	Quality of Task
49	OGN	Open Glider Network
50	OQQ	Quality Assessment Questionnaire
51	SA-UAV	Semi A-UAVs
52	SSQ	Simulation Sickness Questionnaire
53	SA	Situation Awareness
54	SSA	State and Situation Awareness
55	SCS	Simulation and Cyber Sickness
56	SS	Simulation Sickness
57	STT	Safety Travel Tube
58	TL	Transfer Learning
59	TS	Total Score
60	UAV	Unmanned Aerial Vehicle
61	UTM	UAV Traffic Management
62	V2V	Vehicle-to-Vehicle
63	WLAN	Wireless Local Area Network

and the human operator needs not always watch over the system'', ''the human operator must know the status of the system when an urgent event occurs in the system and human intervention is required, or he is asked for some cooperation from agents''. In a similar domain, this subject was extensively focused on during the 2000s while a mass number of robotic applications were taking their indispensable places. Fong et al. [20–23] closely scrutinised this subject and developed a framework in 2003 [21]. In the framework, how a few humans can teleoperate multiple teams of robots to accomplish the targeted task – that is, to assemble large orbital structures – was analysed. Later, human–robot teaming was focused on by Nourbakhsh et al. in 2005 [24] in real-world problem-solving applications, e.g. for urban search and rescue. The research on human–multirobot interaction in many disciplines has increased exponentially to solve real-world problems from the perspectives of HITL and HOTL since these preliminary works. Different types of immersive devices have been developed to interface with remote objects. Today's telemanipulation systems allow the interaction with environments at a distance and can also scale human force and motion to achieve stronger, bigger, or smaller action capabilities [25]. The study by Mithal et al. [26] suggests that joysticks are harder to control than mice. Martins et al. [27] concluded that

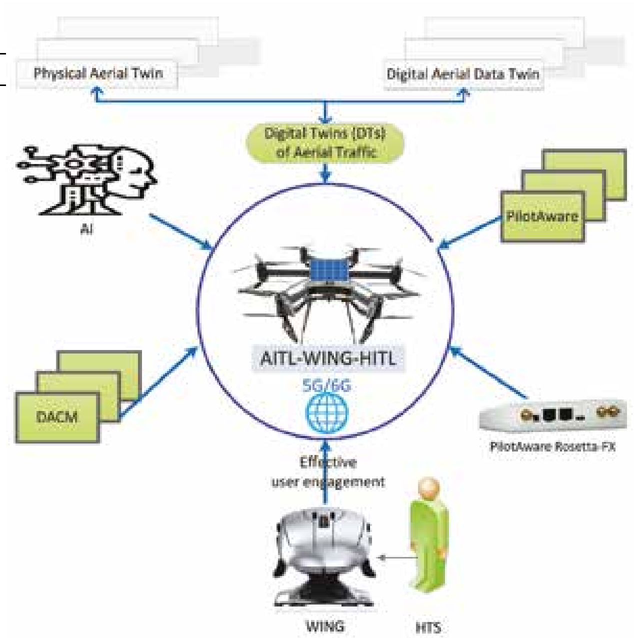

Fig. 2. Main building blocks of AITL-WING-HITL.

Fig. 3. WING device employed for Ground Based WING Station (GBS) using one hand.

participants' (with motor disabilities) feedback was more positive regarding 3D optical mice compared to the use of a conventional keyboard+mouse combination for navigation in 3D environments. The WING was tested in controlling 3D objects within computer-aided design (CAD) applications by Turner et al. [28], and by Sandoval et al. [29] in two short papers and found to be efficient in manipulating 3D virtual objects. Sandoval et al. [30], while testing several input devices with varying DoF, concluded that the more DoF available, the more enhanced the control over objects.

Human–drone interaction has been scrutinised by the research community to build easy-to-use interaction interfaces (e.g. natural interaction interfaces [31,32], touch-based [33]). The real-world telemanipulation initiatives with A-UAVs are expanding within the industry with the use of BVLOS, in particular, within the military industry. The aerial industry is partnering with leading telecommunication and technology companies that are experimenting with remote telemanipulation of A-UAVs in stochastic environments. Advanced multi-agent platforms, as well as hefty devices to interface with these platforms, are required to extend human intelligence and experience for tele co-working with multiple A-UAVs to accomplish tasks as desired. In this sense, existing works on drone manipulation need to be extended to mitigate the aforementioned concerns. To this end, to the best of the observed knowledge, having received limited attention in the literature, telemanipulating A-UAVs through different intervention modes has not been analysed in-depth in the sense of establishing a holistic HITL/HOTL approach for improving co-work between humans and multiple A-UAVs, which makes this paper unique, aiming at closing this gap.

3. Methodology

The integration of A-UAVs into non-segregated UTM+ATM aerospace environments necessitates unified platforms that support collective operations to ensure missions are carried out both efficiently and safely. Such platforms are essential for maintaining coordinated control of multi-DoF aerial vehicles while preserving safe separation distances. During the autonomous execution of multiple UAV missions – often orchestrated by different entities – unexpected events may arise, and individual missions cannot be treated in isolation, as they share the same aerospace infrastructure. This study aims to develop an integrated, collective framework that enables HITL and AITL agents to collaboratively manage uncertainty and execute autonomous missions effectively. The proposed approach supports global BVLOS operations by incorporating a comprehensive State and Situation Awareness (SSA) tracking system. The core components of the proposed platform – AITL-WING-HITL (Fig. 16) – for the manipulation of A-UAVs are illustrated in Fig. 2. At its foundation, the platform integrates the PilotAware system (Supplement II, Fig. 1) and the DACM system (Supplement III, Fig. 2) to generate DTs of aerial traffic. These primary components, along with supporting systems, are detailed in Section 3.1, prior to the full presentation of the developed platform in Section 3.2.

3.1. Background

Recent advances in Cyber-Physical Systems (CPSs) within the concepts of Internet of Everything (IoE) and Automation of Everything (AoE) [34] teleport us to teleoperate remote objects using DTs. In this treatise, the components of the designed platform which are depicted in Fig. 2 are explained in Sections 3.1.1, 3.1.2, 3.1.3, and 3.1.4 respectively and then the platform, as a holistic framework, is examined in 3.2.

3.1.1. WING device

The WING, a mouse-like, precision control device, was developed by Worthington Sharpe Ltd. in order to use the human motor system effectively. It is presented in Figs. 3, 4 with its functions. It, by extending the abilities of a mouse, combines the functions of a free-moving isotonic mouse and a free-flowing isometric joystick, leading to unprecedented freedom of movement from a desk-based control system. It enables movements in X, Y

Fig. 4. Essential attributes: The mapping of the WING to the rotational orientations with three degrees — roll (Φ), pitch (Θ) and yaw (Ψ) channels

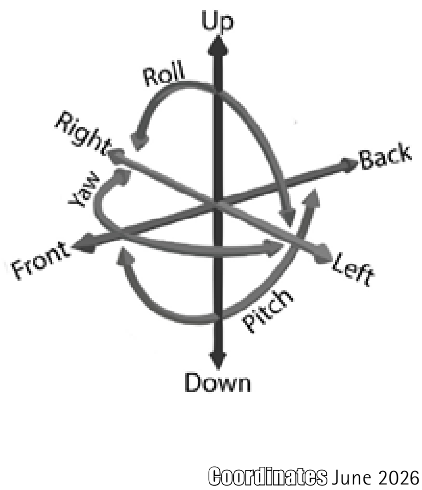

Fig. 5. Conceptualisation of 6DoF (i.e. 3 translation degrees and 3 rotation degrees) of the WING.

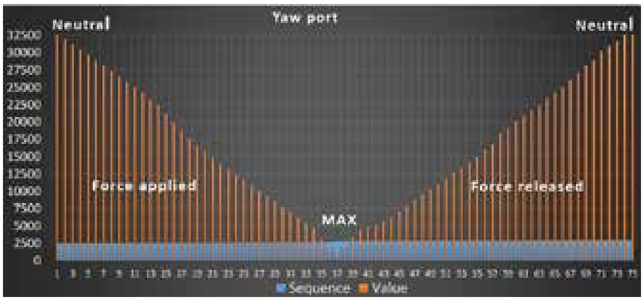

Fig. 6. States of Yaw Port (Table 2).

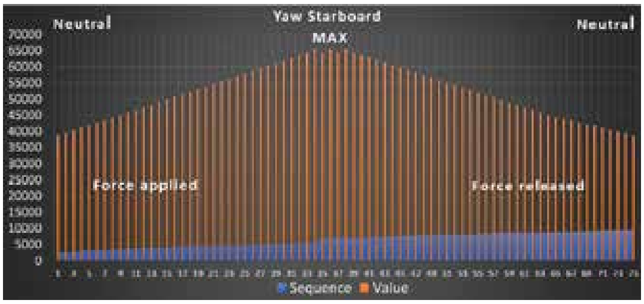

Fig. 7. States of Yaw Starboard (Table 2).

and Z directions as well as a complete precision roll (Φ), pitch (Θ) and yaw (Ψ) joystick functions as delineated in Fig. 5.

The WING aims to create command and control solutions for ROVs and robotic equipment. The lower part contains the laser mouse sensor; the upper part attaches via a precision slide and pivot mechanism to provide pitch, roll and z-height movement. Further control is then added through the under-slung yaw-bar positioned towards the front, giving a total of 6DoF. It, with advanced sensory mechanisms allowing precision control, was designed to address the needs of users who require the speed and accuracy of a high-end mouse for pointing and selection tasks, along with full 3D control. Additionally, it offers a wide range of buttons and a speed wheel that can be further programmed both to perform numerous functions and to map certain actions as we employ in this study. Readers are referred to the video5 to observe how it functions with its particular features. Its particular functionalities regarding the primary objectives of this research can be summarised as follows.

i. Multiple A-UAVs can be hooked and manipulated separately by the same hand.
ii. A-UAVs can be directed using pre-defined navigation waypoints, and their trajectories can be adjusted during the mission.
iii. Integrated 4-axis joystick functionality allows for performing various actions synchronously, such as simultaneous mission planner operation, camera gimbal control, flight path adjustments, or full manual piloting.
iv. Joystick functions can be integrated into APM Planner 2.0, Ardupilot Mission Planer, DJI Ground Station, and any independent Ground Control Station (GCS) that supports standard joystick inputs (Fig. -3).
v. Familiar computer mouse shape, speed, and accuracy

Table 2
Discrete microstructure movement (tele-impedance) of the WING in Yaw channel regarding the time and the subsequent sequences providing more information about the movement velocity over time: Port (Fig. 6); Blackboard (Fig. 7).

N	Yaw Port (RotationZ)			Yaw Starboard (RotationZ)			Force
	Seq	Timestamp	Value	Seq	Timestamp	Value	
1	2495	185 328 531	32 767	2416	266 585 875	38 749	Neutral
2	2496	185 328 537	31 993	2551	266 586 343	39 529	Applied
3	2499	185 328 546	31 219	2668	266 586 734	40 310	Applied
4	2502	185 328 546	30 445	2956	266 587 765	41 090	Applied
5	2503	185 328 562	29 671	3200	266 588 640	41 970	Applied
6	2508	185 328 578	28 897	3209	266 588 671	42 650	Applied
7	2515	185 328 593	28 123	3379	266 589 234	43 430	Applied
8	2520	185 328 609	27 349	3490	266 589 687	44 210	Applied
9	2526	185 328 625	26 575	3579	266 589 984	44 991	Applied
10	2533	185 328 656	25 801	3619	266 590 093	45 771	Applied
11	2537	185 328 671	25 027	3687	266 590 312	46 551	Applied
12	2542	185 328 687	24 253	3841	266 590 843	47 331	Applied
13	2545	185 328 703	23 221	3990	266 591 375	48 111	Applied
14	2548	185 328 718	22 447	4031	266 591 546	49 152	Applied
15	2555	185 328 734	21 141	4056	266 591 656	49 932	Applied
16	2557	185 328 750	19 867	4231	266 592 250	50 712	Applied
17	2559	185 328 750	18 835	4265	266 592 359	51 492	Applied
18	2562	185 328 781	17 545	4323	266 592 562	52 272	Applied
19	2565	185 328 796	16 513	4423	266 592 937	53 052	Applied
20	2566	185 328 796	15 738	4454	266 593 046	53 833	Applied
21	2577	185 328 828	14 706	4579	266 593 406	54 613	Applied
22	2582	185 328 843	13 932	4642	266 593 656	55 393	Applied
23	2589	185 328 875	13 158	4671	266 593 750	56 173	Applied
24	2601	185 328 906	12 384	4685	266 593 812	57 213	Applied
25	2606	185 328 921	11 610	4834	266 594 312	57 993	Applied
26	2610	185 328 937	10 836	4882	266 594 500	58 774	Applied
27	2618	185 328 953	10 062	4907	266 594 593	59 554	Applied
28	2621	185 328 968	9288	5069	266 595 125	60 334	Applied
29	2625	185 329 000	8514	5075	266 595 156	61 114	Applied
30	2632	185 329 015	7740	5086	266 595 187	61 894	Applied
31	2638	185 329 031	6966	5091	266 595 203	62 674	Applied
32	2647	185 329 062	6192	5416	266 596 406	63 455	Applied
33	2654	185 329 093	5418	5425	266 596 468	64 235	Applied
34	2662	185 329 125	4644	5428	266 596 468	65 275	Applied
35	2669	185 329 156	3096	7021	266 602 234	64 495	Applied
36	2676	185 329 187	2322	7024	266 602 250	65 275	Applied
37	2750	185 329 468	1548	7026	266 602 250	64 495	END
38	2828	185 329 687	2322	7031	266 602 281	65 275	Released
39	2832	185 329 703	3354	7047	266 602 343	64 495	Released
40	2833	185 329 718	4386	7094	266 602 531	63 715	Released
41	2836	185 329 726	4782	7188	266 602 890	62 934	Released
42	2839	185 329 734	5160	7197	266 602 906	62 154	Released
43	2841	185 329 742	5676	7203	266 602 937	61 374	Released
44	2843	185 329 750	6192	7526	266 604 062	60 594	Released
45	2847	185 329 765	6966	7638	266 604 453	59 814	Released
46	2856	185 329 781	7998	7694	266 604 671	59 034	Released
47	2860	185 329 796	8772	7795	266 605 015	58 253	Released
48	2864	185 329 812	9546	7837	266 605 140	57 473	Released
49	2868	185 329 812	10 320	7867	266 605 250	56 693	Released
50	2870	185 329 828	11 094	7904	266 605 390	55 913	Released
51	2873	185 329 828	11 868	7976	266 605 703	55 133	Released
52	2881	185 329 859	12 642	8066	266 606 015	54 353	Released
53	2886	185 329 875	13 416	8135	266 606 250	53 572	Released
54	2890	185 329 890	14 190	8148	266 606 296	52 792	Released
55	2896	185 329 906	14 964	8337	266 606 953	52 012	Released
56	2900	185 329 921	15 996	8389	266 607 125	51 232	Released
57	2903	185 329 921	16 771	8517	266 607 593	50 452	Released
58	2907	185 329 937	18 319	8591	266 607 859	49 672	Released
59	2911	185 329 953	19 093	8617	266 607 953	48 891	Released
60	2912	185 329 953	20 125	8619	266 607 968	48 111	Released
61	2913	185 329 968	20 899	8623	266 607 984	47 331	Released
62	2914	185 329 968	21 673	8627	266 608 000	46 551	Released
63	2915	185 329 984	22 447	8638	266 608 031	45 771	Released
64	2920	185 330 000	23 479	8659	266 608 093	44 991	Released
65	2922	185 330 015	24 253	8890	266 608 890	44 210	Released
66	2925	185 330 015	25 027	8912	266 589 687	43 918	Released
67	2931	185 330 046	26 059	8948	266 609 093	43 430	Released
68	2932	185 330 046	27 091	8961	266 609 125	42 650	Released
69	2934	185 330 062	28 123	8997	266 609 317	42 112	Released
70	2935	185 330 062	28 897	9049	266 609 437	41 870	Released
71	2937	185 330 078	30 187	9183	266 609 906	41 090	Released
72	2939	185 330 078	30 961	9254	266 610 187	40 310	Released
73	2940	185 330 078	31 735	9271	266 610 221	39 910	Released
74	2941	185 330 093	32 767	9287	266 610 312	39 529	Released
75	2942	185 331 062	32 767	9296	266 610 343	38 749	Neutral

reduce the learning curve, allowing the operator to focus on the task promptly during telemanipulation.

The min and max values of the rotational orientations — roll (Φ), pitch (Θ) and yaw (Ψ) are shown in Table 3. The WING's motions with discrete microstructure values can be mapped into the manoeuvres of A-UAVs. The Yaw states of the WING detected by the developed application in this research are shown in Table 2, and their graphical representations are depicted in Fig. 6 for Yaw Port and Fig. 7 for Yaw Starboard. The acquired sequences and the time are incorporated to visualise how the velocity varies over the duration of the force applied and released. The readers are referred to Supplement I for all the translated input forces (Fig. 4) into sub-movement microstructure states.

3.1.2. Vehicle autonomy, AITL, HITL, HOTL, and HOOTL

The exponential growth of interest and research in UAVs is strongly pushing for the emergence of autonomous flying robots [35]. 10 control levels of UAV swarms from fully supervisor-controlled to fully autonomous mode between human and machine were analysed in [36]. Drone Industry Insights (DRONEII) categorises the autonomy with 5 levels [37] based on degrees of independence, namely, 1: low automation (i.e. the UAV has control of at least one vital function, with a pilot in control); 2: partial automation (i.e. the UAV can take over heading and altitude under certain conditions with a pilot still responsible for safe operation); 3: conditional automation (i.e. the UAV can perform all functions and a pilot acts as a fall-back system); 4: high automation (i.e. the UAV has back-up systems, so if one fails, the platform is still operational while a pilot is out of the loop); 5: full automation (i.e. the UAV can plan its actions using advanced AI learning techniques) with little to no human intervention in the control loop. As the level of autonomy increases, UAVs can operate in more complex environments and execute more complex tasks with less prior knowledge and fewer operator interactions [38].

Table 3
WING min and max values of the rotational orientations — roll (Φ), pitch (Θ) and yaw (Ψ).

Orientation	WING	WING State	Min/Max	Parameter	Value
Yaw (Ψ)	Yaw Port	RotationZ	Max	Ψ_{Pmax} =	32 767
Yaw (Ψ)	Yaw Port	RotationZ	Min	Ψ_{Pmin} =	1548
Yaw (Ψ)	Yaw Starboard	RotationZ	Max	Ψ_{Smax} =	64 495
Yaw (Ψ)	Yaw Starboard	RotationZ	Min	Ψ_{Smin} =	38 749
Roll (Φ)	Roll Port	X	Max	Φ_{Pmax} =	60 074
Roll (Φ)	Roll Port	X	Min	Φ_{Pmin} =	37 189
Roll (Φ)	Roll Starboard	X	Max	Φ_{Smax} =	36 149
Roll (Φ)	Roll Starboard	X	Min	Φ_{Smin} =	3870
Pitch (Θ)	Pitch Forward	Y	Max	Θ_{Fmax} =	37 709
Pitch (Θ)	Pitch Forward	Y	Min	Θ_{Fmin} =	10 836
Pitch (Θ)	Pitch Backward	Y	Max	Θ_{Bmax} =	62 414
Pitch (Θ)	Pitch Backward	Y	Min	Θ_{Bmin} =	39 790

AI agents are now capable of intentionally constraining, complementing, or substituting human involvement in the execution of routine tasks [39]. With Human-out-of-the-Loop (HOOTL) systems, AI agents are expected to execute assigned tasks without human intervention. Humans and machines may need to work hand-in-hand to complete numerous tasks safely, accurately, efficiently, and ethically, in particular, for safety-critical jobs requiring a high level of precision. HITL interaction, requiring active human involvement, is employed for the systems by which a task may not be achieved either by a human or a machine. The concept of HITL dates back to the early 1940s, when humans primarily served as error detectors, monitoring systems and intervening when necessary [40]. HITL, i.e. hands-on, system allows humans to monitor the actions continuously, interact with the system and manipulate decisions that do not seem to be an optimal outcome or situations that involve nondeterministic behaviours of AI. SA-UAVs require humans (HITL) and onboard AI (AITL) to interact with each other continuously, where uncertainty is possible to emerge. In other words, there is always a person or people watching the HITL system actively, in which SA-UAVS are mainly involved, to intervene to fix any problem that is expected to occur. On the other hand, there is no need to employ a person to monitor FA–UAVS. However, it‘s still best to have a person as HOTL passively for remote monitoring to easily step in when alerted by the AI agent and manipulate when autonomy – AITL –encounters uncertainty about what to do next. HOTL interaction turns into HITL when the human agent is alerted. However, HITL is a phase that continues until an alerted uncertainty is handled, and the system turns into the HOTL interaction after the job has been completed. In 2025, the London Office of Technology and Innovation (LOTI) launched a research project to explore the role of HITL, prompted by ongoing questions about what constitutes meaningful human involvement and how effective the designated individual is in mitigating the ethical risks associated with AI [41]. Generally speaking, HOTL/HITL systems are utilised to ensure the expected automated behaviour of A-UAVs and consequently to ensure aerial traffic safety as well as ground-based safety. HOTL systems, while operating with little to no human intervention and not requiring to be alerted all the time, still allow HTMs to perform other tasks while the autonomy level of decentralised agents is relied on to accomplish assigned missions/tasks. HTMs monitor A-UAVs during the progress of the assigned missions within the HITL system. HITL, where a HTM is supposed to be on alert all the time to fix any emerging problem that the vehicle cannot cope with, is commonly used in controlling level-3 and level-4 autonomy. A level-5 autonomy can perform under all predefined circumstances and conditions. In this regard, this paper focuses on both HOTL and HITL with A-UAVs, where the HTM is expected to intervene remotely in rare difficulties that the vehicle cannot tackle under exceptional conditions.

Table 4
Data Streaming from the PilotAware system: Instant flight information. The value of the instant data capture in time, epoch (i.e. Unix timestamp), 162 522 6964, equals “Fri Jul 02 2021 12:56:04 GMT+0100 British Summer Time”.

	Time (epoch)	Transponder	Receiver	Latitude	Longitude	Altitude (Feet)	Heading	Speed (knots/h)	Call sign
Example 1	162 522.964	401B8D	ADB	52.08688	0.170053	1100	237	88	GBCOU

Fig. 8. PilotAware small lightweight Rosetta-FX graffiti module, combining all EC technologies together and enabling seamless Flarm Integration, can detect all EC types including ADS-B, Sky Echo, PilotAware, Mode-S with Weather RADAR and Enhanced Traffic Data

Fig. 9. Generation of future waypoints: safety travel tube with estimationbased predictive display

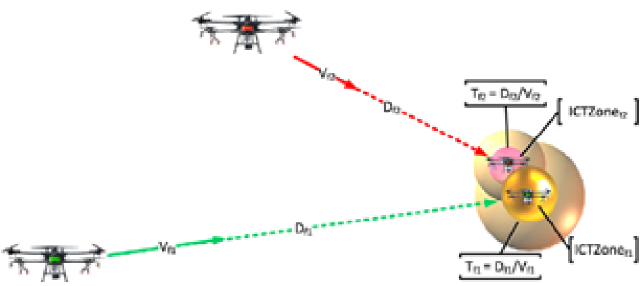

Fig. 10. Estimation-based predictive display: Early warning for a collision risk concerning an impending crossing point (impending crossing within $IcRz$) with two flights that have different velocities and are flying at similar altitudes. V, D and T correspond to "velocity", "distance" and "time to reach the crossing point" respectively.

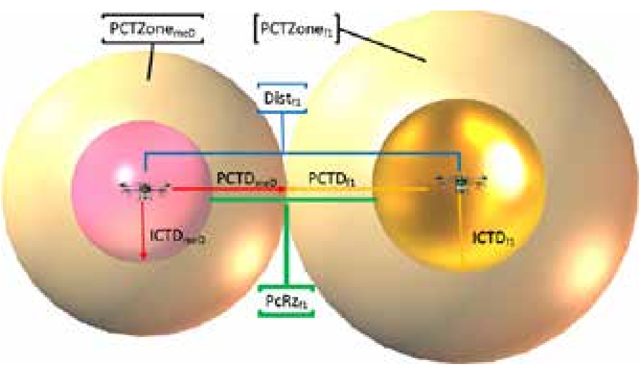

Fig. 11. Alert-YELLOW: Conflict geometry of $PCTD$ and $P\ cRz$: The yellow zone for each flight represents $PCTZone$. The red zone for meD and the orange zones for other flights represent $ICTZones$. (For interpretation of the references to colour in this figure legend, the reader is referred to the web version of this article.)

Autonomy has changed the relationship between humans and robots extensively. They are becoming more harmonious while taking part in specific task executions as the level of autonomy increases with further intelligence. This relationship is elaborated in Section 3.2.1 with various intervention modes. It must be noted that the HOTL/HITL manipulation through the intervention modes is performed if necessary, and AITL is expected to take over the HTM completely as soon as possible to realise the main objective of autonomy – self-reliance and self-governing (see Fig. 8 for the EC device and Table 4 for a data instance example acquired from the EC device).

3.1.3. PilotAware ATOM-GRID Network

The PilotAware ATOM-GRID Network (i.e. currently over 320 UK ATOM stations) is elaborated in Supplement II. The network detects aircraft that transmit any of the various Electronic Conspicuity (EC) signals used in Europe. These include ADS-B (Automatic Dependent Surveillance-Broadcast), CAP 1391 and Mode-S signals on the ICAO (International Civil Aviation Organisation) aviation band and Flarm, PilotAware, Fanet + and OGN (Open Glider Network) trackers that use the EASA (European Union Aviation Safety Agency) SRD 860 Band. Aircraft that transmit using the SafeSky mobile app are also detected.

3.1.4. DACM (Drone Aware Collision Management) system

The DACM system was developed to monitor aerial traffic and trigger autonomous cooperative manoeuvres that consider the aerodynamic, flight dynamics and particular features (e.g. physics, kinematics, manoeuvrability) of A-UAVs as mobile aerial agents within a multi-disciplinary joint project [42]. This system is illustrated in Supplement III (Fig. 2). The interface of this system, equipped with simulation capabilities and low-cost equipment, provides us with a full range of testing capabilities in both real-world applications of A-UAVs and co-simulation environments. The DACM – that is tightly coupled with the PilotAware ATOM-GRID Network (Section 3.1.3) – collects instant operational manoeuvre information from all aerial vehicles via simultaneous

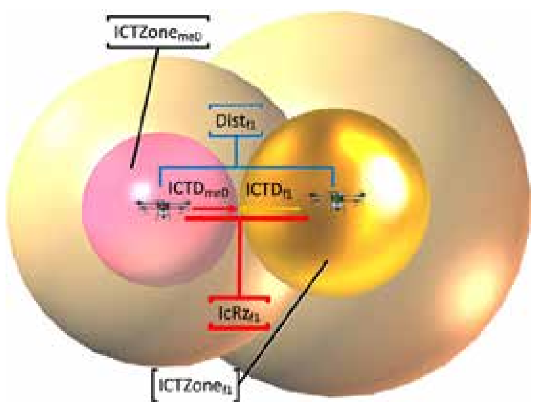

Fig. 12. High-alert-RED: Conflict geometry of $ICTD$ and $IcRz$.

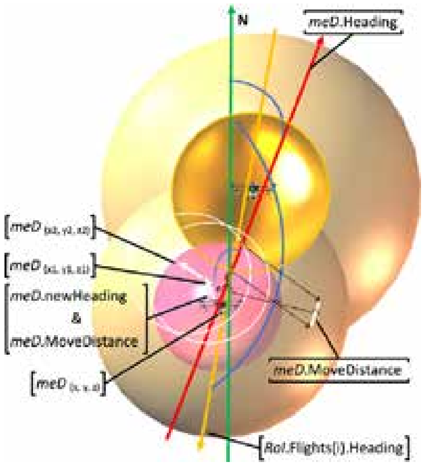

Fig. 13. Geometric illustration of CA manoeuvres (Supplement III, Alg. 2). $meD.MoveDistance$ **is corresponding to the invasion length of the** $ICTZones$**.**

Fig. 14. Self manoeuvring using the simulated and real flight data: Red $ICTZone$ **and heading and yellow** $PCTZone$ **within the original path; white** $ICTZone$ **and heading and blue** $PCTZone$ **within the manoeuvring trajectory. (For interpretation of the references to colour in this figure legend, the reader is referred to the web version of this article.)**

low-bandwidth data streams from each of the aerial vehicles. The low-bandwidth dual-path data communication is also mainly used in this research for conveying HTM command messages (e.g. new_heading = heading + 15) and necessary telemetry data (e.g. battery level of A-UAVs). The DACM – a digital replica of aerial traffic – integrates all near-real-time streamed data within its DT counterpart for convenient monitoring with more immersive telepresence for HTMs. Autonomous actuation for A-UAVs is performed to avoid emerging hazards in this immersive interface. The DACM supports HTMs to perceive the remote aerial traffic with effective SSA. The main features are outlined as follows.

1) The DACM, equipped with a novel CM methodology within an autonomy control framework using geometry formation of flights, enables BVLOS operations with collision-free trajectories.
2) The system, with (i) perception, (ii) decision-making, and (iii) automated actuation phases, can perceive the surrounding dynamic environment precisely using a global coverage strategy requiring no sophisticated sensors and react efficiently to multiple non-linear collision risks at a time with minimum trajectory deviations, requiring no prior training.
3) The DACM in both air-only and air/ground modes not only implements Collision Avoidance (CA) for FA-UAVs, but also manages Pilot-Controlled UAVs (PC-UAVs) in improving operational safety, where it might be difficult for pilots to detect surrounding close-range/high-speed flights (see Fig. 13 for the geometric illustration of CA manoeuvres).

$$\begin{aligned} PcRz_{f1} &==> (Dist_{f1} \leq PCTD_{meD} + PCTD_{f1}) \ \& \\ &(Dist_{f1} > ICTD_{meD} + ICTD_{f1}); \\ &where\,(0 < P_c \leq 0.5) \ \& \ (PCTD = 2 \ X \ ICTD) \end{aligned} \quad (1)$$

$$\begin{aligned} IcRz_{f1} &==> (Dist_{f1} \leq ICTD_{meD} + ICTD_{f1}) \ \& \ (Dist_{f1} > 0); \\ &where \quad (0.5 < P_c \leq 1) \ \& \ (PCTD = 2 \ X \ ICTD); \end{aligned} \quad (2)$$

$$\begin{aligned} ICTZone &= \frac{4}{3}\pi(ICTD)^3; \\ PCTZone &= (\frac{4}{3}\pi(PCTD)^3) - ICTZone = \frac{28}{3}\pi(ICTD)^3; \end{aligned} \quad (3)$$

$$\begin{aligned} \textbf{CALatR} &= \sin^{-}\ (\sin(latR) * \cos(distCARadius) \\ &+ \cos(latR) * \sin(distCARadius) * \cos(bearingCAR)); \\ \textbf{CALonR} &= LonR + \tan^{-1}(\sin(bearingCAR) * \sin(distCARadius) \\ &* \cos(latR))/(\cos(distCARadius) - \sin(latR) * \sin(meCALat)); \\ \underline{\textbf{meDCALat}} &= CALatR * (180/\pi); \underline{\textbf{meDCALon}} = CALonR * (180/\pi); \\ \textbf{where}\, latR &= meLat * (\pi/180); lonR = meLon * (\pi/180); \\ bearingCAR &= newHeading * (\pi/180); \\ distCARadius &= MoveDistance/EarthRadius; \end{aligned} \quad (4)$$

The modules of the DACM, allowing autonomous navigation for A-UAVs with appropriate actuation mechanisms by coordinating the actions of multiple heterogeneous A-UAVs, are introduced in Supplement III, and the methodology using these modules is depicted in Supplement III (Fig. 2). In addition to autonomous actuation mechanisms to avoid any collision risk, the DACM system alerts the HOTL/HITL HTM if any flight is departing from its pre-planned trajectory, where the two control inputs (i.e. pre-planned waypoints and active waypoints) do not agree, considering that a probable failure is causing this unexpected manoeuvre under no collision risk using the health assessment and failure detection module.

The main goal of CM is to keep flights away from hazardous regions with conflict-free solutions at the very early stage by keeping each flight well clear of other traffic, considering their current trajectories and preplanned routes. Currently, A-UAVs do not have a system that will warn an operator of an impending collision with other airborne vehicles [43] using broader local coverage. In this module, SSA through horizontal and vertical planes is provided with the active flights and early collision risk assessment is processed, considering their trajectory predictions. From a linear formulation technical viewpoint, the flights' time-invariant connectivity of previous waypoints, their trajectory headings and their Probable Collision Travel Cone ($P\ CT\ Zone$) and Imminent Collision Travel Zones ($ICT\ Zones$) are used to

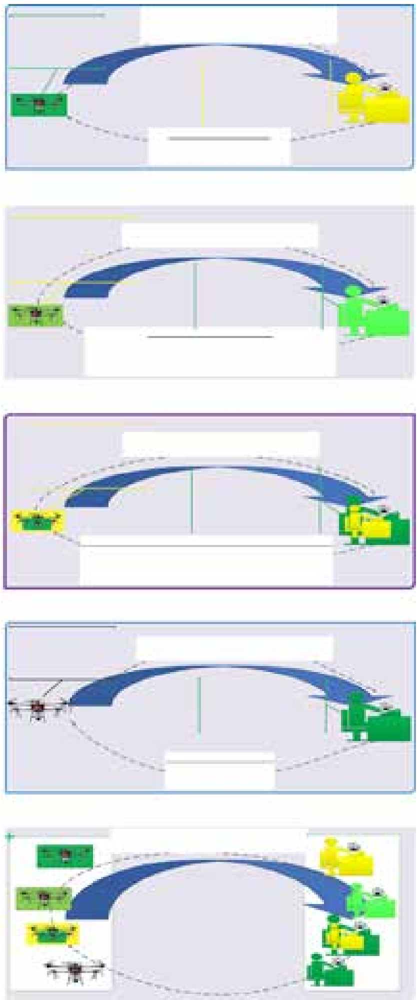

Fig. 15. HITL/HOTL interaction with a high level of transparency. Intervention modes: "No-control (supervisory)", "co-activity (shared)", "collaboration (joint)", "full control (master–slave)", and "cooperation (all togetherness)".

generate the projections of future linear or non-linear waypoints (e.g. kinematic Cartesian Virtual Points (CVPs)), leading to a Safety Travel Tube (STT) using an estimation-based predictive display as depicted in Fig. 9. A-UAVs are said to be within Flight of Safety Route, i.e. $FoSR$, where there are no overlapping STTs as shown in Fig. 10 with estimation-based predictive directions. The DACM is responsible for instructing the flight controller, i.e. HTM, to maintain A-UAV separation from conflicting regions with a conflict resolution mechanism and to avoid imminent collisions autonomously. The HTM with HOTL mode is first informed about the approaching collision risk if STTs of flights are intersecting at a crossing point, considering the conflict geometry regarding the velocities, heading and altitudes. The system turns into the HITL state, where there is a crossing point indicating an impending collision risk. The system, second, warns for the probable collision risks (within Probable-collision-Risk zone ($PcRz$)) as illustrated in Fig. 11. Third, it alerts for imminent collision risks (within Imminent-collision-Risk zone ($IcRz$)) as illustrated in Fig. 12 along with autonomous deconflicting manoeuvres (Fig. 14).

3.2. AITL-WING-HITL platform

Fatigue, lack of concentration, and poor displays all contribute to reduced performance in telemanipulating remote objects, and humans have difficulty building mental models of remote environments [20]. Therefore, these shortcomings must be compensated for with the establishment of easy-to-use interfaces, enabling robust interaction between AITL AI agents and remote human cognitive intelligence. Most importantly, two intelligent nodes – A-UAV and skilled HTM – have to be tightly coupled with human-oriented and vehicle-centric interfaces by exploiting the smartness at the vehicle end. The remote environment of A-UAVs should be observed by HTMs using constant dynamic SSA to generate proper commands at the appropriate time.

The AITL-WING-HITL platform aims to provide a tightly coupled interface between two intelligent agents — HOTL/HITL HTM and onboard aerial AITL AI agent from a multi-agent manipulation perspective. It encompasses a variety of human–robot co-work technologies that enable various interaction modes (elaborated in Section 3.2.1) and guarantee seamless transitions between these modes whenever they are needed. Technically speaking, the platform provides the HTM with a high degree of immersiveness ability with the established DTs of aerial traffic to enable the HTM to both perfectly perceive the remote aerial traffic with a full sense of telepresence (e.g. transparency) and track the results of their manipulated discrete microstructure actuation (i.e. teleimpedance) with back-feeding by incorporating a large set of integrated components as shown in Fig. 2. These integrated components mainly allow the user to interact with precision (e.g. correct aerial information with the PilotAware network (Supplement II, Fig. 1)), real-time user tracking of aerial traffic supported by a large set of proactive AI implementations (e.g. early warning, CA) with the DACM (Supplement III (Fig. 2)) and 6DoF in manipulation with the WING (Figs. 4, 5) as well as its discrete microstructure movement (Figs. 6, 7, Table 2). First, we would like to examine the co-work aspects of two intelligent entities theoretically through different intervention modes (Fig. 15) in Section 3.2.1 before delving into the merits of AITL-WING-HITL in Section 3.2.2.

3.2.1. Intervention modes within AITL-WING-HITL

A-UAVs operate autonomously and need to receive assistance whenever necessary. Time-varying delays are inevitable during the co-work interaction regarding the communication time delay problem, decision-making delays regarding the Quality of Experience (QoE) of HTMs and the evaluation of the voluminous sensor data and actuation time delays; Moreover, human remote intervention is vulnerable to human decision errors regarding incomplete environmental information based on the current state and imminent states of the vehicle concerning the other traffic participants, obstacles and hazards [8]. Even with a high level of SSA, human telemanipulation is strictly dependent on the cognitive and perceptual capabilities, spatial orientation abilities and motor skills of HTMs to avoid risky manoeuvres [8]. To this end, it is important to use the intelligence at the remote site, and it is advantageous to co-work during the execution of the complex tasks that cannot be handled by autonomy.

If A-UAVs are capable of performing on their own, human intervention is not needed, allowing HOTL systems, particularly with FA–UAVs. Otherwise, a remote extension of human intelligence and expertise with HITL interaction may be necessary either for better task performance to avoid disastrous situations during possibly hazardous operations or for executing very complex tasks beyond the capabilities of autonomy. The WING, with 6DoF, allows a HTM, with superior motor capabilities and perception/interpretation/implementation skills, to have partial or total control of A-UAVs to achieve their tasks safely and efficiently. With the help of the WING, HITL HTM inputs range with discrete microstructure values as depicted in Table 2, considering the intervention modes ranging from ‘‘no-control (supervisory) mode’’ to ‘‘full-control (master–slave) teleoperation mode’’ as delineated in Fig. 15. These intervention modes are elaborated in our previous study in [44]. These modes are summarised below in their dedicated subsections. The WING allows a HTM to switch between AITL and HITL states as well as between the interaction modes. The AITL-WING-HITL platform provides HTMs and AI agents with a high level of transparency through these interaction modes to work together with a high degree of efficacy. The WING, interfaced with AITL-WING-HITL, coordinates the tasks/subtasks by effectively modulating the HTM's hand tele-impedance in a smooth, goal-oriented manner based on the required behaviours of the intervention mode in action and the task to be accomplished. The HTM with the HOTL interaction mode can change the state to HITL to monitor the aerial traffic at any time and take action in one of the intervention modes to ascertain aerial safety or to accomplish any particular tasks. Then, the HITL state can be switched to the HOTL state after any uncertainty is managed successfully. The following intervention modes are analysed within the AITL-WING-HITL framework when continued assistance is critical for A-UAVs.

No-control (supervisory) mode (Fig. 15A): it is a time where the AI can empirically be proved to be on such a high degree of superiority that the human's input may affect the task performance negatively. The involvement of HTMs is aimed to be minimised in this mode. The HTM, as a task-specific HITL, encourages the A-UAV in a non-decisive mood to take either one of the options determined by the vehicle itself or a different predetermined option.

Co-activity (shared-control) mode (Fig. 15B): Some tasks may not be achieved by allocating sub-task responsibilities distinctively between the HTM and A-UAVs, which may lead to compromising task performance. Combining human and robot skills via intelligent interfaces seems very appealing; in this manner, establishing principled co-activity methods to seamlessly blend the control between the human and the robot to enable the combined system to surpass both the robot and human performance with reduced human effort is a prime goal for robotics [45]. This mode assists both intelligent agents – HITL HTM and AITL AI – in achieving the common goal safely.

Collaboration (joint-control or traded control) mode (Fig. 15C): AI-located/assigned series of fine-grained sub-tasks need to be performed individually either by the AITL or HITL agent. Neither the HTM is in full control of the A-UAV nor the A-UAV is in full control of itself, where various specific sub-tasks are allocated between the HTM and A-UAV beforehand. The control is traded back and forth to execute fine-granular sub-tasks, enabling joint problem-solving. Partial control can be mainly used for tightly coupled coordination between collocated HTM and A-UAVs to achieve joint task performance, wherever difficulty that cannot be coped with by the autonomy is alerted. Instead of a supervisor dictating to a subordinate, the human and the robot engage in dialogue to exchange ideas and resolve differences in the collaborative mode [23]. This mode aims to produce a better outcome than either the human or A-UAV performs alone.

Table 5
Main distinctive features of the intervention modes.

	Loop	Decision	Obedience A-UAV	Obedience HTM	Solution for conflicts	Full control	Built-in safety mechanism
No-control (supervisory)	HITL	HTM	Yes	No	N/A	Yes (A-UAV)	Operational
co-activity (shared-control)	HITL & AITL	HTM & A-UAV	No	Yes	HTM & A-UAV	No	Operational
Collaboration (joint-control)	HITL || AITL	HTM || A–UAV	No	No	HTM || A-UAVs	Partial	Operational
Full-control	HITL	HTM	Yes	No	N/A	Yes (HTM)	Inactive
Cooperation (all togetherness)	Mix interactions	Mix modes (above)	Mix modes (Yes || No)	Mix modes (Yes || No)	Mix modes (above)	Mix modes(above)	Operational

Table 6
Transition responsibilities for the intervention mode switching.

Switching decision	Current control	Next control	Current dominance	Next dominance	Switching control
No » » co-activity	A-UAV	A-UAV-HTM	A-UAV	A-UAV&HTM	A-UAV
No » » collaboration	A-UAV	A-UAV-HTM	A-UAV	HTM	A-UAV&HTM
No » » full	A-UAV	A-UAV-HTM	A-UAV	HTM	A-UAV&HTM
Co-activity » » collaboration	A-UAV-HTM	A-UAV-HTM	A-UAV&HTM	HTM	HTM
Co-activity » » full	A-UAV-HTM	A-UAV-HTM	A-UAV&HTM	HTM	HTM
Co-activity » » no	A-UAV-HTM	A-UAV	A-UAV&HTM	A-UAV	A-UAV
Collaboration » » full	A-UAV-HTM	A-UAV-HTM	HTM	HTM	HTM
Collaboration » » no	A-UAV-HTM	A-UAV	HTM	A-UAV	HTM&A-UAV
Collaboration » » co-activity	A-UAV-HTM	A-UAV-HTM	HTM	A-UAV&HTM	HTM
Full » » no	A-UAV-HTM	A-UAV	HTM	A-UAV	HTM&A-UAV
Full » » co-activity	A-UAV-HTM	A-UAV-HTM	HTM	A-UAV&HTM	HTM
Full » » collaboration	A-UAV-HTM	A-UAV-HTM	HTM	HTM	HTM

Full-control (master–slave) mode (Fig. 15D): Complete task may need to be performed by the HTM alone under extreme conditions in this mode. The HTM, as a leading agent, takes over the control and leads the A-UAV as a follower agent. Different from the collaboration mode, the A-UAV, piloted remotely by the HTM, obeys the manoeuvres performed by the HTM under any circumstances.

Cooperation (all togetherness) mode Swarms of A-UAVs sometimes need to interact with each other to accomplish a single task faster than a single A-UAV or to solve difficult tasks that are beyond a single A-UAV's capability, where each A-UAV assists in the accomplishment of the desired goal, considering its specific capabilities, e.g. carrying a very heavy payload together with a robotic arm or a suspended cable grasped by a fixed gripper, search and rescue by assigning different target Region of Interest (RoI) to multiple A-UAVs.

The main distinctive features of the intervention modes are summarised in Table 5. A merge of these intervention modes can be employed by switching from one mode to another for specific parts of a complicated task to cope with highly difficult challenges. Switching decisions between modes can be determined based on the characteristics and dominance of the modes as presented in Table 6. For instance, the switching decision for "from no-control to co-activity and then to collaboration and then to full-control and then again back to no-control" is controlled and carried out by A-UAV, HTM, HTM and "HTM & A-UAV together" respectively.

3.2.2. Modules, techniques, & interface of AITL-WING-HITL

The main components of the AITL-WING-HITL platform (Fig. 2) are already explained in the related sections of this paper above in Sections Section 3.1.1, 3.1.2, 3.1.3, and 3.1.4. Therefore, we will be focusing on the particular characteristics of the platform in this section to reveal the specific features that are gained from the mould of the aforementioned components. A-UAVs have diverse characteristics, and they are designed with particular features and onboard equipment concerning the missions they are expected to perform [7]. In this regard, the manipulation of different types of A-UAVs requires particular control parameters representing the particular features of A-UAVs. The HTM can manipulate the speed, altitude, and heading of A-UAVs, considering the other aerial vehicles in the environment both to avoid instant collisions and not to cause new collision risks with the generated manoeuvres as illustrated in Fig. 16E.1. Commands generated through the WING are transformed to the hooked A-UAVs using the off-the-shelf drone controlling systems such as UgCS, DJI (Fig. 16E.2.) as elaborated in our previous research in [42].

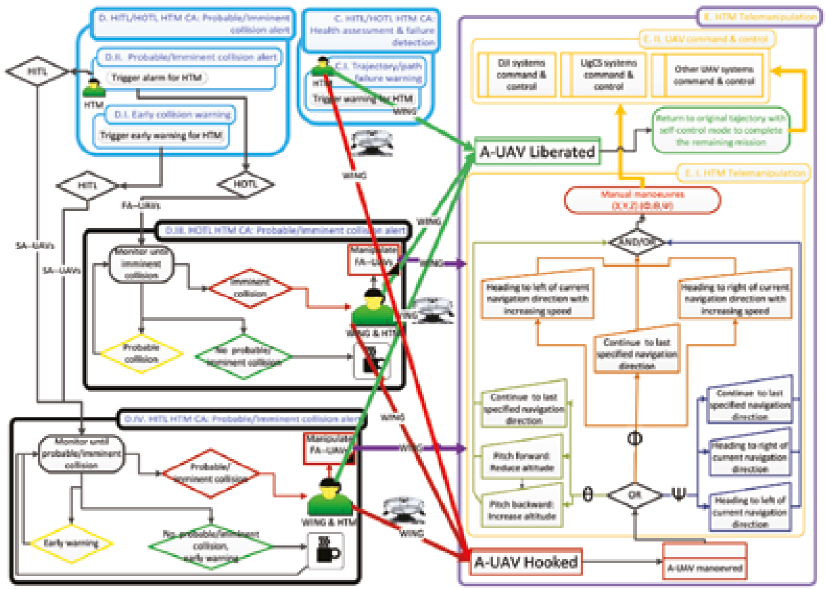

Fig. 16. Methodology of hooking and manipulation of A-UAVs using the WING. The part human intervention, D.1 (Algorithm 1), in this figure is replaced with the autonomous intervention part, D.1, in the DACM system in Supplement III (Fig. 2) when A-UAVs are manipulated by HTMs with the inputs from C.III (HOTL) and C.IV (HITL) (Algorithm 1). (For interpretation of the references to colour in this figure legend, the reader is referred to the web version of this article.)

Fig. 17. Interface of the AITL-WING-HITL platform. (For interpretation of the references to colour in this figure legend, the reader is referred to the web version of this article.)

Interface of the AITL-WING-HITL platform: The AITL-WING-HITL application provides an improved, easy-to-use Graphical User Interface (GUI) for manipulating A-UAVs in the specified aerial zone using the WING, leading to fine-granular force, direction, and amplitude. The interfaces of intelligent systems are supposed to be considered to reduce the cognitive load to the possible minimum complexity, paving the way for effective human intervention with a high degree of perception. In this direction, the interface of AITL-WING-HITL was designed to be as simple as possible by avoiding HTMs with unnecessary overwhelming information. Additionally, it, as displayed in Fig. 17, provides HTMs with effective perception capabilities which allow HTMs to focus on the particular sections of the interface with which they are supposed to interact. For instance, the colour of an A-UAV's heading line turns black when that UAV is suggested to the HTM to be hooked and manipulated during a collision risk. The circles of $P\ CT\ Zone$ and $ICT\ Zone$ turn black to show that the A-UAV is hooked by the HTM for manipulation. The primary interface elements are (i) DTs of aerial traffic, (ii) the WING that is coupled between HTMs and A-UAVs within DTs, (iii) the interactive interface control elements and (iv) informative elements. Either the HITL agent or the AITL agent determines the intervention mode and transitions between these modes as outlined in Table 6. Either with a button click on the WING or with a selection from the interactive interface control elements, the HTM can switch between the interaction states (i.e. HOTL and HITL) and the intervention modes, namely, no-control (supervisory), co-activity (shared-control), collabo-ration (joint-control), full-control (master–slave), and cooperation (all togetherness) (Fig. 15).

Hooking with WING (Fig. 16C.1, D.III, D.IV): HTMs may need to intervene in the current actions of A-UAVs for better task performance or to avoid hazards. The flights that indicate a collision risk are highlighted in the interface, and the system turns into HITL state from HOTL state. A HTM can hook one of these flights using the immersive device to manipulate its actions. The interface may suggest that a specific A-UAV shall be hooked and manipulated during a collision risk by turning its heading line black. More specifically, the system can recommend a specific A-UAV to be hooked if there is a collision risk between that A-UAV and Manned Aerial Vehicles (MAVs), where there is no possibility to hook MAVs. Similarly, fixed-wing drones are recommended by the system against rotary-wing drones, while the battery constraint feature of rotary-wing drones is evident. In the same manner, the fixed-wing drone with a stronger battery level is advised over the other fixed-wing drone with a lower battery level, whereas rotary-wing drones with stronger battery levels are proposed against other rotary-wing drones with lower battery levels. Moreover, drones with an air-based mission against drones with a ground-based mission are selected by the system for hooking, where drones with air-based missions are not required to turn to their leaving point at the original trajectory. Likewise, the slower drone can be recommended against the faster one, while the manoeuvring may be easier with the slower drone. The circles of the $P\ CT\ Zone$ and $ICT\ Zone$ turn black to denote that the A-UAV is hooked by the HTM for manipulation.

The hooking of a specific A-UAV takes place when the WING-Button-1-clicked point is within the $ICT\ Zone$ of the A-UAV. The HTM remains in the manipulation mode until the hooking is released using the WING-Button-2-clicked point in the same way. The $ICT\ Zone$, $P\ CT\ Zone$, and the heading turn into black colour (Fig. 17) to signify the hooked A-UAVs during the manipulation phase. The HTM can hook and manipulate multiple A-UAVs simultaneously. While an A-UAV is implementing the last command in the hooked state, e.g. heading to a new direction with a new altitude, the HTM can hook other A-UAVs to manipulate their actions. In this way, multiple A-UAVs can be hooked, which means that they no longer implement their preplanned way-points, velocity, and altitude while the WING is actively manipulating another drone. The actuation per A-UAV is performed using one of the intervention modes (Fig. 15) explained in Section 3.2.1. The liberated A-UAVs from the hooking state return to their original trajectory using the shortest path to implement their pre-planned missions.

Manipulation of A-UAVs with WING (Fig. 16E.1): The mobile Internet with low-latency and high bandwidth capabilities, enabling access to information on an anywhere-anytime basis, has democratised our life in many aspects, in particular, providing fast remote operation abilities [8]. Telepresence of HTMs within aerial traffic is provided by the AITL-WING-HITL platform. The WING offers an intuitive way of controlling multiple degrees of freedom (i.e. multiple axes) simulta-neously, aiming at using the human motor system effectively with a higher information capacity. One hand is in manipulating A-UAVs; the other hand is free to operate aircraft systems through the keyboard or the control panel of the AITL-WING-HITL platform. The mapping of the values acquired from the WING to drone manoeuvres is shown in Algorithm 1. This mapping actuates the hooked A-UAVs appropriately as illustrated in Fig. 16E.1. The user can choose the proper intervention mode within the interface and can translate the inputs of the WING into a particular transfer function that manipulates A-UAVs accordingly. HTMs are immersed with A-UAVs through force/torque applied or released to the rotational orientations — roll (Φ), pitch (Θ) and yaw (Ψ) channels (Fig. 4). The buttons on the WING are employed to switch between several states and actuation functions. The use of the buttons in hooking and releasing A-UAVs is explained earlier.

The SSA of aerial traffic is constantly generated using the global SSA strategy implemented by the PilotAware system (Section 3.1.3). The movements of aerial vehicles are computed by the DACM (Section 3.1.4). The DACM triggers alarms and warnings when the AITL agent experiences a difficult situation or there is a hazard, such as impending collision risks, beforehand for the HTM to take action and manipulate A-UAVs remotely. The HTM within the UTM+ATM system is authorised to intervene in the autonomous actions of A-UAVs. The HTM can adjust the position (longitudinal and lateral), altitude, angular velocity and orientation of A-UAVs concerning their environments with a quick response using the WING. It is worth emphasising that drones can be manipulated with desired navigational actions, considering the dynamic characteristics of the aerial environment and the particular drone physics-based rules defined in the system, such as manoeuvrability, velocity, and acceleration. In this sense, interactions between HTMs and A-UAVs differ depending on the capabilities of A-UAVs. For instance, a drone can accelerate to its maximum allowable speed, but not above it, even if it is forced to a velocity that is above the maximum defined speed. The discrete microstructure values of 6DoF (x, v, z, Ψ, Θ, Φ) (Fig. 5), corresponding to the geospatial orthogonal axes (i.e. three state variables — translational coordinates (x, v, z) and rotational coordinates (Ψ, Θ, Φ), are mapped to the manoeuvrers of A-UAVs. The translational coordinates are very much dependent on the angular coordinates in our model as formulated in Algorithm 1. Taking this into consideration, the maximum manoeuvrability of the A-UAVs is determined according to the yaw, pitch and roll orientation as ($-\pi \leqslant \Psi \leqslant \pi$), ($-\pi/2 \leqslant \Theta \leqslant \pi/2$), and ($-\pi/2 \leqslant \Phi \leqslant \pi/2$). The A-UAV changes its trajectory as the HTM applies the desired force on the WING. The A-UAV follows the latest action taken by the HTM if the HTM releases the force completely. In other words, the A-UAV follows the heading with specified altitude and velocity directed by the HTM, even though the WING leaves the drone for manipulating other A-UAVs for the sake of simplicity, assuming that the HTM is not required to hold the WING actions at a specific trajectory for a specific drone. In this way, multiple A-UAVs can be hooked simultaneously. The A-UAV follows similar actions continuously, where the HTM applies the maximum allowed force on the device. For instance, the heading can change to the left or right of the original direction by 15∘, which results in a circular trajectory. The relationship between the inputs and outputs is managed by mapping interactions' inputs to desired outcomes concerning the particular manoeuvrability capabilities of each A-UAV. The number of actions in the specified direction (i.e. roll (Φ), pitch (Θ) and yaw (Ψ)) executed by an A-UAV, leading to the change of rotation angles of the X, Y, and Z axis is dependent on the DoF, the number of sequences executed by the HTM and their values and timestamps (e.g. Table 2, Figs. 6, 7). The hooked drone has to co-work with the HTM by following the actions directed by the HTM to increase its task performance and avoid hazardous situations. The platform reacts to any imminent collision risk. An imminent collision risk can be caused if any required desired action is not actuated by the HTM within the early warning zone (Fig. 10) and the $PcRz$ (Fig. 11) despite the system collision warnings and alarms, which may lead to making drones meet in the $IcRz$ (Fig. 12). An imminent collision risk can also be caused by the instant actions of the HTM during the implementation of any intervention modes. The WING has a significant degree of inertia, which may cause the HTM to overshoot their desired location or move too fast. To avoid unexpected manoeuvres based on the fast-changing microstructure of the WING with a sequence of multiple sub-movements, the directions of the selected intervention mode within 6DoF are taken into consideration along with the

Algorithm 1: Manipulation of A-UAVs (Fig. 16E.1) using the WING device.

```
Data: System input: Ψ_Pmax & Ψ_Pmin & Ψ_Smax & Ψ_Smin & Φ_Pmax & Φ_Pmin & Φ_Pmax & Φ_Pmin & Θ_Fmax & Θ_Fmin & Θ_Bmax & Θ_Bmin (Table 3)
Data: Instant input: RoI.flights.Data
Result: D_H.Ψ & D_H.Φ & D_H.Θ & D_H.heading & D_H.speed & D_H.alt
=> Create the hooked drone for manipulation & initialise variables;
HookedDrone D_H = new HookedDrone(); D_H = meD;
Φ_prev = 0; Θ_prev= 0; Ψ_prev = 0;D_H.Φ = 0; D_H.Θ = 0; D_H.Ψ = 0;
=> Inputs from WING;
while hooked do
    if ((W_s == "RotationZ")&&((D_H.Ψ > −π)||(D_H.Ψ < π))) then
        => Assign the WING value to Yaw (Ψ);
        Ψ_cur = W_val;
        if (((Ψ_cur < Ψ_Pmax)&&(Ψ_cur < Ψ_prev))||(Ψ_cur == Ψ_Pmin)) then
            => Heading to left of the current navigation direction;
            D_H.heading = D_H.heading - D_H.property(Ψ_DiffDeg);
            D_H.Ψ = D_H.Ψ - D_H.property(Ψ_DiffDeg);
        else if (((Ψ_cur > Ψ_Pmin)&&(Ψ_cur > Ψ_prev))||(Ψ_cur == Ψ_Pmax)) then
            => Heading to right of the current navigation direction;
            D_H.heading = D_H.heading + D_H.property(Ψ_DiffDeg);
            D_H.Ψ = D_H.Ψ + D_H.property(Ψ_DiffDeg);
        else
            => Continue to last specified navigation direction;
        end
        navigateD_H (D_H.Ψ, D_H.Φ, D_H.Θ, D_H.heading, D_H.speed, D_H.alt);
        Ψ_prev = Ψ_cur;
    else if ((W_s == "X")&&((W_val < Φ_Smax)||(W_val > Φ_Pmin))&&((D_H.Φ > −π/2)||(D_H.Φ < π/2))) then
        => Assign the WING value to Roll (Φ);
        Ψ_cur = W_val;
        if (((Φ_cur < Φ_Smax)&&(Φ_cur < Φ_prev))||(Φ_cur == Φ_Smin)) then
            => Roll starboard: Heading to left of current navigation direction with increasing speed;
            D_H.heading = D_H.heading - D_H.property(Φ_DiffDeg);
            D_H.speed = D_H.speed + D_H.property(Φ_DiffDeg);
            D_H.Φ = D_H.Φ - D_H.property(Φ_DiffDeg);
        else if (((Φ_cur > Φ_Pmin)&&(Φ_cur > Φ_prev))||(Φ_cur == Φ_Pmax)) then
            => Roll port: Heading to right of current navigation direction with increasing speed;
            D_H.heading = D_H.heading + D_H.property(headDiff);
            D_H.speed = D_H.speed + D_H.property(speedDiff);
            D_H.Φ = D_H.Φ + D_H.property(Φ_DiffDeg);
        else
            => Continue to last specified navigation direction;
        end
        navigateD_H (D_H.Ψ, D_H.Φ, D_H.Θ, D_H.heading, D_H.speed, D_H.alt);
        Φ_prev = Φ_cur;
    else if ((W_s == "Y")&&((W_val < Θ_Fmax)||(W_val > Θ_Bmin))&&((D_H.Θ > −π/2)||(D_H.Θ < π/2))) then
        => Assign the WING value to pitch (Θ);
        Ψ_cur = W_val;
        if (((Θ_cur < Θ_Fmax)&&(Θ_cur < Θ_prev))||(Θ_cur == Θ_Fmin)) then
            => Pitch forward: Reduce altitude;
            D_H.alt = D_H.alt - D_H.property(altDiff);
            D_H.speed = D_H.speed - D_H.property(speedDiff);
            D_H.Θ = D_H.Θ - D_H.property(Θ_DiffDeg);
        else if (((Θ_cur > Θ_Bmin)&&(Θ_cur > Θ_prev))||(Θ_cur == Θ_Bmax)) then
            => Pitch backward: Increase altitude;
            D_H.alt = D_H.alt + D_H.property(altDiff);
            D_H.speed = D_H.speed - D_H.property(speedDiff);
            D_H.Θ = D_H.Θ + D_H.property(Θ_DiffDeg);
        else
            => Continue to last specified navigation direction;
        end
        navigateD_H (D_H.Ψ, D_H.Φ, D_H.Θ, D_H.heading, D_H.speed, D_H.alt); Θ_prev = Θ_cur;
    else
        => Return to original trajectory after released from hooking;
        hooked = "false";
        ReturnToOriginalTrajectory();
    end
end
```

capabilities of the drones in manipulation. This provides the user with the means to limit movement with more resistance.

A HTM can be cautioned with an alert by the AITL AI agent about the emerging situation. Telemanipulation requests and intervention requirements can be prioritised by the HTM or the system, and several of these can be commanded to take an idle safe position or trajectory (e.g. a circular trajectory as mentioned above) without endangering the vehicle itself and surrounding traffic by hooking multiple A-UAVs simultaneously. They can be handled later in priority scheduling order or hazard states (i.e. red, yellow, green) by a HTM, enabling task allocation. This property enables a single HTM with limited sensorimotor capabilities to manage a large area with heavy aerial traffic.

Liberation of A-UAVs and their return to the original trajectory (Fig. 16C.1, D.III, D.IV): A specific drone can be released from hooking when the WING-Button-2-clicked point is within the $ICT\ Zone$ of the A-UAV. The circles denoting $ICT\ Zone$, $P\ CT\ Zone$, and the heading line turn into their original colour from black (Fig. 17) after the A-UAV is liberated to indicate that they are performing their tasks independently with the AITL agent themselves. A-UAVs orient themselves in Euclidean space by means of the preplanned trajectory after being released from the hook, considering their physical manoeuvring features and the instant SSA environmental inputs.

The paper is originally published in Robotics and Autonomous Systems, Volume 202, 2026.

The paper is republished with authors' permission. https://doi.org/10.1016/j.robot.2026.105486.

To be concluded in next issue.

References

[1] NewYorkTimes, A successful exhibition of electrical transmission without wires in the garden, 1898.
[2] T.K. Sarkar, R. Mailloux, A.A. Oliner, M. Salazar-Palma, D.L. Sengupta, History of Wireless, Wiley, NJ, USA, 2006.
[3] N. Tesla, Method of and apparatus for controlling mechanism of moving vessels or vehicles, 1898, U.S. Patent US613809A.
[4] J. Turi, Tesla's toy boat: A drone before its time, 2014.
[5] K. Kuru, D. Ansell, W. Khan, H. Yetgin, Analysis and optimization of unmanned aerial vehicle swarms in logistics: An intelligent delivery platform, IEEE Access 7 (2019) 15804–15831, http://dx.doi.org/10.1109/ACCESS.2019.2892716.
[6] K. Kuru, W. Khan, A framework for the synergistic integration of fully autonomous ground vehicles with smart city, IEEE Access 9 (2021) 923–948, http://dx.doi.org/10.1109/ACCESS.2020.3046999.
[7] K. Kuru, Planning the future of smart cities with swarms of fully autonomous unmanned aerial vehicles using a novel framework, IEEE Access 9 (2021) 6571–6595, http://dx.doi.org/10.1109/ACCESS.2020.3049094.
[8] K. Kuru, Conceptualisation of human-on-the-loop haptic teleoperation with fully autonomous self-driving vehicles in the urban environment, IEEE Open J. Intell. Transp. Syst. 2 (2021) 448–469, http://dx.doi.org/10.1109/OJITS.2021. 3132725.
[9] J.M. Bradshaw, V. Dignum, C. Jonker, M. Sierhuis, Human-agent-robot team- work, IEEE Intell. Syst. 27 (2) (2012) 8–13, http://dx.doi.org/10.1109/MIS.2012.37.
[10] M. Chowdhury, M. Maier, Toward dynamic hart-centric task offloading over fiwi infrastructures in the tactile internet era, IEEE Commun. Mag. 57 (11) (2019) 123–128, http://dx.doi.org/10.1109/MCOM.001.1800669.
[11] Y. Li, Trends in control and decision-making for human–robot collaboration systems [bookshelf], IEEE Control Syst. Mag. 39 (2) (2019) 101–103, http://dx.doi.org/10.1109/MCS.2018.2888714.
[12] M. Shahbazi, S.F. Atashzar, R.V. Patel, A systematic review of multilateral teleoperation systems, IEEE Trans. Haptics 11 (3) (2018) 338–356, http://dx. doi.org/10.1109/TOH.2018.2818134.
[13] W.R. Ferrell, T.B. Sheridan, Supervisory control of remote manipulation, IEEE Spectr. 4 (10) (1967) 81–88, http://dx.doi.org/10.1109/MSPEC.1967.5217126.
[14] K. Kuru, Trustfsdv: Framework for building and maintaining trust in self- driving vehicles, IEEE Access 10 (2022) 82814–82833, http://dx.doi.org/10.1109/ACCESS.2022.3196941.
[15] V.R. Garate, S. Gholami, A. Ajoudani, A scalable framework for multi-robot tele-impedance control, IEEE Trans. Robotics 37 (6) (2021) 2052–2066, http://dx.doi.org/10.1109/TRO.2021.3071530.
[16] Y. Nakauchi, T. Okada, N. Yamasaki, Y. Anzai, Multi-agent interface architecture for human–robot cooperation, in: Proceedings 1992 IEEE International Conference on Robotics and Automation, Vol. 3, 1992, pp. 2786–2788, http://dx.doi.org/10.1109/ROBOT.1992.220012.
[17] T. Laengle, T. Hoeniger, L. Zhu, Cooperation in human–robot-teams, in: ISIE'97 proceeding of the IEEE International Symposium on Industrial Electronics, Vol. 3, 1997, pp. 1297–1301, http://dx.doi.org/10.1109/ISIE.1997.648935.
[18] T. Suzuki, K. Yokota, H. Asama, H. Kaetsu, I. Endo, Cooperation between the human operator and the multi-agent robotic system: evaluation of agent monitoring methods for the human interface system, in: Proceedings 1995 IEEE/RSJ International Conference on Intelligent Robots and Systems. Human Robot Interaction and Cooperative Robots, Vol. 1, 1995, pp. 206–211, http://dx.doi.org/10.1109/IROS.1995.525798, vol.1.
[19] T. Fujita, H. Kimura, The design of software development system for multiple robots, in: Proceedings of 1993 IEEE/RSJ International Conference on Intelligent Robots and Systems, IROS'93, Vol. 2, 1993, pp. 1119–1125, http://dx.doi.org/10.1109/IROS.1993.583331, vol.2.
[20] T. Fong, S. Grange, C. Thorpe, C. Baur, Multi-robot remote driving with collaborative control, in: Proceedings 10th IEEE International Workshop on Robot and Human Interactive Communication. ROMAN 2001 (Cat. No. 01TH8591), 2001, pp. 237–242, http://dx.doi.org/10.1109/ROMAN.2001.981908.
[21] T. Fong, C. Thorpe, C. Baur, Multi-robot remote driving with collaborative control, IEEE Trans. Ind. Electron. 50 (4) (2003) 699–704, http://dx.doi.org/10.1109/TIE.2003.814768.
[22] T.W. Fong, C. Thorpe, C. Baur, Advanced interfaces for vehicle teleoperation: Collaborative control, sensor fusion displays, and remote driving tools, Auton. Robot.: Spec. Issue Teleoperation Interfaces 11 (1) (2001) 77–85.
[23] T.W. Fong, Collaborative Control: A Robot-Centric Model for Vehicle Tele-operation (Ph. D. thesis), Carnegie Mellon University, Pittsburgh, PA, 2001.
[24] I. Nourbakhsh, K. Sycara, M. Koes, M. Yong, M. Lewis, S. Burion, Human–robot teaming for search and rescue, IEEE Pervasive Comput. 4 (1) (2005) 72–79, http://dx.doi.org/10.1109/MPRV.2005.13.
[25] S. Hirche, M. Buss, Human-oriented control for haptic teleoperation, Proc. IEEE 100 (3) (2012) 623–647, http://dx.doi.org/10.1109/JPROC.2011.2175150.
[26] A.K. Mithal, S.A. Douglas, Differences in movement microstructure of the mouse and the finger-controlled isometric joystick, in: Proceedings of the SIGCHI Conference on Human Factors in Computing Systems, CHI'96, Association for Computing Machinery, New York, NY, USA, 1996, pp. 300–307, http://dx.doi. org/10.1145/238386.238533.
[27] M. Martins, A. Cunha, L. Morgado, Usability test of 3dconnexion 3d mice versus keyboard+mouse in second life undertaken by people with motor disabilities due to medullary lesions, Procedia Comput. Sci. 14 (2012) 119–127, http://dx.doi.org/10.1016/j.procs.2012.10.014, Proceedings of the 4th International Conference on Software Development for Enhancing Accessibility and Fighting Info-exclusion (DSAI 2012).
[28] M.J. Turner, T. Morris, M. Sandoval, 12DoF Interaction for Scientific Visualisation, in: T.R. Wan, F. Vidal (Eds.), Computer Graphics and Visual Computing, The Eurographics Association, 2017, http://dx.doi.org/10.2312/cgvc.20171274.
[29] M. Sandoval, Multiple Degrees-of-Freedom Input Devices for Interactive Command and Control Within Virtual Reality in Industrial Visualizations (Ph.D. thesis), Department of Computer Science, The University of Manchester, Manchester, UK, 2023.
[30] M. Sandoval, T. Morris, M. Turner, Controlling 3D visualisations with multiple degrees of freedom, in: F.P. Vidal, G.K.L. Tam, J.C. Roberts (Eds.), Computer Graphics and Visual Computing, CGVC, The Eurographics Association, 2019,http://dx.doi.org/10.2312/cgvc.20191263.
[31] R.A. Suárez Fernández, J.L. Sanchez-Lopez, C. Sampedro, H. Bavle, M. Molina, P. Campoy, Natural user interfaces for human-drone multi-modal interaction, in:
2016 International Conference on Unmanned Aircraft Systems, ICUAS, 2016, pp.
1013–1022, http://dx.doi.org/10.1109/ICUAS.2016.7502665.
[32] E. Peshkova, M. Hitz, B. Kaufmann, Natural interaction techniques for an unmanned aerial vehicle system, IEEE Pervasive Comput. 16 (01) (2017) 34–42, http://dx.doi.org/10.1109/MPRV.2017.3.
[33] P. Abtahi, J.L.E.D.Y. Zhao, J.A. Landay, Drone near me: Exploring touch- based human-drone interaction, Proc. ACM Interact. Mob. Wearable Ubiquitous Technol. 1 (3) (2017) http://dx.doi.org/10.1145/3130899.
[34] K. Kuru, H. Yetgin, Transformation to advanced mechatronics systems within new industrial revolution: A novel framework in automation of everything (aoe), IEEE Access 7 (2019) 41395–41415, http://dx.doi.org/10.1109/ACCESS.2019.2907809.
[35] S. Bouabdallah, M. Becker, R. Siegwart, Autonomous miniature flying robots: coming soon! - research, development, and results, IEEE Robot. Autom. Mag. 14 (3) (2007) 88–98, http://dx.doi.org/10.1109/MRA.2007.901323.

[36] G. Coppin, F. Legras, Autonomy spectrum and performance perception issues in swarm supervisory control, Proc. IEEE 100 (3) (2012) 590–603, http://dx.doi.org/10.1109/JPROC.2011.2174103.
[37] M. Radovic, Tech talk: Untangling the 5 levels of drone autonomy, 2019.
[38] K. Nonami, Present state and future prospect of autonomous control technology for industrial drones, IEEJ Trans. Electr. Electron. Eng. 15 (1) (2020) 6–11, http://dx.doi.org/10.1002/tee.23041,arXiv:https://onlinelibrary.wiley.com/doi/pdf/10.1002/tee.23041.
[39] A. Murray, J. Rhymer, D.G. Sirmon, Humans and technology: Forms of conjoined agency in organizations, Acad. Manag. Rev. 46 (3) (2021) 552–571, http://dx. doi.org/10.5465/amr.2019.0186.
[40] M. Anderson, K. Fort, Human where? a new scale defining human involvement in technology communities from an ethical standpoint, Int. Rev. Inf. Ethics 31 (1) (2022).
[41] M. Say, Loti looks at 'humans in the loop' in ai deployments, 2025.
[42] K. Kuru, J.M. Pinder, B.J. Watkinson, D. Ansell, K. Vinning, L. Moore, C. Gilbert, A. Sujit, D. Jones, Toward mid-air collision-free trajectory for autonomous and pilot-controlled unmanned aerial vehicles, IEEE Access 11 (2023) 100323–100342, http://dx.doi.org/10.1109/ACCESS.2023.3314504.
[43] R.W. Osborne, Y. Bar-Shalom, P. Willett, G. Baker, Design of an adaptive passive collision warning system for uavs, IEEE Trans. Aerosp. Electron. Syst. 47 (3) (2011) 2169–2189, http://dx.doi.org/10.1109/TAES.2011.5937290.
[44] K. Kuru, Human-in-the-loop telemanipulation schemes for autonomous unmanned aerial systems, in: 2024 4th Interdisciplinary Conference on Electrics and Computer, INTCEC, 2024, pp. 1–6, http://dx.doi.org/10.1109/INTCEC61833.2024.10603071.
[45] N. Amirshirzad, A. Kumru, E. Oztop, Human adaptation to human–robot shared control, IEEE Trans. Hum.–Mach. Syst. 49 (2) (2019) 126–136, http://dx.doi.org/10.1109/THMS.2018.2884719.
[46] N. Dużmańska, P. Strojny, A. Strojny, Can simulator sickness be avoided? A review on temporal aspects of simulator sickness, 9, 2018, http://dx.doi.org/10.3389/fpsyg.2018.02132,
[47] R.S. Kennedy, N.E. Lane, K.S. Berbaum, M.G. Lilienthal, Simulator sickness questionnaire: An enhanced method for quantifying simulator sickness, Int. J. Aviat. Psychol. 3 (3) (1993) 203–220, http://dx.doi.org/10.1207/s15327108ijap0303_3, arXiv:https://doi.org/10.1207/s15327108ijap0303_3.
[48] K. Brunnström, E. Dima, T. Qureshi, M. Johanson, M. Andersson, M. Sjöström, Latency impact on quality of experience in a virtual reality simulator for remote control of machines, Signal Process., Image Commun. 89 (2020) 116005, http://dx.doi.org/10.1016/j.image.2020.116005.
[49] K. Kuru, Telemanipulation of autonomous drones using digital twins of aerial raffic, 2024, http://dx.doi.org/10.21227/kn5m-z290.
[50] C. Jay, M. Glencross, R. Hubbold, Modeling the effects of delayed haptic and visual feedback in a collaborative virtual environment, ACM Trans. Comput.-Hum.Interact. 14 (2) (2007) 8–es, http://dx.doi.org/10.1145/1275511.1275514.
[51] C. Jay, R. Hubbold, Delayed visual and haptic feedback in a reciprocal tapping task, in: First Joint Eurohaptics Conference and Symposium on Haptic Interfaces for Virtual Environment and Teleoperator Systems. World Haptics Conference, 2005, pp. 655–656, http://dx.doi.org/10.1109/WHC.2005.29.
[52] J.D. Moss, E.R. Muth, Characteristics of head-mounted displays and their effects on simulator sickness, Hum. Factors 53 (3) (2011) 308–319, http://dx.doi.org/10.1177/0018720811405196, PMID: 21830515. arXiv:https://doi.org/10.1177/0018720811405196.
[53] B.-C. Min, S.-C. Chung, Y.-K. Min, K. Sakamoto, Psychophysiological evaluation of simulator sickness evoked by a graphic simulator, Appl. Ergon. 35 (6) (2004) 549–556, http://dx.doi.org/10.1016/j.apergo.2004.06.002.
[54] J. Lee, M. Kim, J. Kim, A study on immersion and vr sickness in walking interaction for immersive virtual reality applications, Symmetry 9 (5) (2017) http://dx.doi.org/10.3390/sym9050078.
[55] S.V.G. Cobb, S. Nichols, A. Ramsey, J.R. Wilson, Virtual reality-induced symptoms and effects (vrise), Presence: Teleoper. Virtual Env. 8 (2) (1999) 169–186, http://dx.doi.org/10.1162/105474699566152.
[56] K. Desai, S. Raghuraman, R. Jin, B. Prabhakaran, Qoe studies on interactive 3d tele-immersion, in: 2017 IEEE International Symposium on Multimedia, ISM, 2017, pp. 130–137, http://dx.doi.org/10.1109/ISM.2017.27.
[57] IEEE Standard for Transparency of Autonomous Systems, IEEE Std 7001–2021, 2022, pp. 1–54, http://dx.doi.org/10.1109/IEEESTD.2022.9726144.
[58] K. Sjoberg, P. Andres, T. Buburuzan, A. Brakemeier, Cooperative intelligent transport systems in Europe: Current deployment status and outlook, IEEE Veh. Technol. Mag. 12 (2) (2017) 89–97.
[59] N. Lyamin, A. Vinel, D. Smely, B. Bellalta, Etsi dcc: Decentralized congestion control in c-its, IEEE Commun. Mag. 56 (12) (2018) 112–118.
[60] O. Punal, C. Pereira, A. Aguiar, J. Gross, Experimental characterization and modeling of rf jamming attacks on vanets, IEEE Trans. Veh. Technol. 64 (2) (2015) 524–540.
[61] S. Sekander, H. Tabassum, E. Hossain, Multi-tier drone architecture for 5g/b5g cellular networks: Challenges and trends and prospects, IEEE Commun. Mag. 56 (3) (2018) 96–103.
[62] M. Gharibi, R. Boutaba, S.L. Waslander, Internet of drones, IEEE Access 4 (2016) 1148–1162, http://dx.doi.org/10.1109/ACCESS.2016.2537208.
[63] B. Goldfain, P. Drews, C. You, M. Barulic, O. Velev, P. Tsiotras, J.M. Rehg, Autorally: An open platform for aggressive autonomous driving, IEEE Control Syst. Mag. 39 (1) (2019) 26–55, http://dx.doi.org/10.1109/MCS.2018.2876958.
[64] K. Kuru, Definition of multi-objective deep reinforcement learning reward functions for self-driving vehicles in the urban environment, IEEE Trans. Veh. Technol. 11 (2024) 1–12.
[65] K. Kuru, Management of geo-distributed intelligence: Deep insight as a service (DINSaaS) on forged cloud platforms (FCP), J. Parallel Distrib. Comput. 149 (2021) 103–118, http://dx.doi.org/10.1016/j.jpdc.2020.11.009
[66] Kuru, K., Worthington, S., Ansell, D., Pinder, J.M., Sujit, A., Watkinson, B.J., Vinning, K., Moore, L., Gilbert, C., Jones, D., Tinker-Mill, C., 2026. AITL-WING-HITL: Telemanipulation of autonomous drones using Digital Twins of aerial traffic interfaced With WING. Robotics and Autonomous Systems 202, 105486.
[67] Kuru, K., 2023. Metaomnicity: Toward immersive urban metaverse cyberspaces using smart city digital twins. *Ieee Access*, *11*, pp.43844-43868.
[68] Kuru, K. and Ansell, D., 2020. TCitySmartF: A comprehensive systematic framework for transforming cities into smart cities. *IEEE access*, *8*, pp.18615-18644.
[69] Kuru, K., 2022. Trustfsdv: Framework for building and maintaining trust in self-driving vehicles. *IEEe Access*, *10*, pp.82814-82833.
[70] Kuru, K. and Khan, W., 2018. Novel hybrid object-based non-parametric clustering approach for grouping similar objects in specific visual domains. *Applied Soft Computing*, *62*, pp.667-701.
[71] Kuru, K., Clough, S., Ansell, D., McCarthy, J. and McGovern, S., 2023. WILDetect: An intelligent platform to perform airborne wildlife census automatically in the marine ecosystem using an ensemble of learning techniques and computer vision. *Expert Systems with Applications*, *231*, p.120574.
[72] Kuru, K., Clough, S., Ansell, D., McCarthy, J. and McGovern, S., 2023. Intelligent airborne monitoring of irregularly shaped man-made marine objects using statistical Machine Learning techniques. *Ecological Informatics*, *78*, p.102285.

[73] Kuru, K., Erogul, O. and Xavier, C., 2021. Autonomous low power monitoring sensors. *Sensors*, *21*.
[74] Kuru, K., Ansell, D., Jones, D., Watkinson, B., Pinder, J.M., Hill, J.A., Muzzall, E., Tinker-Mill, C.L., Stevens, K. and Gardner, A., 2024, October. Intelligent airborne monitoring of livestock using autonomous uninhabited aerial vehicles. In *The 11th European Conference on Precision Livestock Farming* (pp. 1100-1110). European Conference on Precision Livestock Farming (ECPLF).
[75] Kuru, K., 2023. Definition of multi-objective deep reinforcement learning reward functions for self-driving vehicles in the urban environment. *IEEE Transactions on Intelligent Transportation Systems*.
[76] Kuru, K. and Kuru, K., 2025. UMetaBE-DPPML: Urban metaverse & blockchain-enabled decentralised privacy-preserving machine learning verification and authentication with metaverse immersive devices. *Internet of Things and Cyber-Physical Systems*, *5*, pp.47-86.
[77] Kuru, K., 2023. Sensors and sensor fusion for decision making in autonomous driving and vehicles.
[78] K. Kuru *et al*., "Platform to Test and Evaluate Human-in-the-Loop Telemanipulation Schemes for Autonomous Unmanned Aerial Systems," *2024 20th IEEE/ASME International Conference on Mechatronic and Embedded Systems and Applications (MESA)*, Genova, Italy, 2024, pp. 1-8, doi: 10.1109/MESA61532.2024.10704856.
[79] Kuru, K., Ansell, D., Jon Watkinson, B., Jones, D., Sujit, A., Pinder, J.M. and Tinker-Mill, C.L., 2023. Intelligent automated, rapid and safe landmine and unexploded ordnance (uxo) detection using multiple sensor modalities mounted on autonomous drones. *IEEE Transactions on Instrumentation and Measurement*.
[80] Kuru, K., 2023, October. Use of autonomous uninhabited aerial vehicles safely within mixed air traffic. In *Global Conference on Electronics, Communications and Networks (GCECN2024)*.
[81] Kuru, K. and Kuru, K., 2024, September. Blockchain-enabled privacy-preserving machine learning authentication with immersive devices for urban metaverse cyberspaces. In *2024 20th IEEE/ASME International Conference on Mechatronic and Embedded Systems and Applications (MESA)* (pp. 1-8). IEEE.
[82] Kuru, K., 2024. Technical report: Analysis of intervention modes in human-in-the-loop (hitl) teleoperation with autonomous unmanned aerial systems.
[83] Kuru, K., 2024. Technical report: Big data-concepts, infrastructure, analytics, challenges and solutions.
[84] Kuru, K., 2014, June. A Novel Hybrid Clustering Approach for Unsupervised Grouping of Similar Objects. In *International Conference on Hybrid Artificial Intelligence Systems* (pp. 642-653). Cham: Springer International Publishing.
[85] Lowe, J. and Kuru, K., 2024, September. Development of machine intelligence for self-driving vehicles through video capturing. In *2024 20th IEEE/ASME International Conference on Mechatronic and Embedded Systems and Applications (MESA)* (pp. 1-8). IEEE.
[86] Kuru, K., 2024. Telemanipulation of autonomous drones using digital twins of aerial traffic.
[87] Kuru, K., 2024, September. Joint cognition of remote autonomous robotics agent swarms in collaborative decision-making & remote human-robot teaming. In *The Premium Global Conclave and Expo on Robotics & Automation (AUTOROBO, EXPO2024)(Session: Robotics Swarm Intelligence)*.
[88] Kuru, K., 2024. Technical report: Human-in-the-loop telemanipulation platform for automation-in-the-loop unmanned aerial systems.
[89] Kuru, K., Ansell, D., Jones, D., Watkinson, B., Pinder, J.M. and Tinker-Mill, C., 2024. Deployment of autonomous IoT drones for precision farming in an automated manner.
[90] Lowe, J. and Kuru, K., 2024, October. Development of Machine Intelligence for Fully Autonomous Ground Vehicles Via Video Analysis. In *2024 20th IEEE/ASME International Conference on Mechatronic and Embedded Systems and Applications (MESA)* (pp. 1-8). Institute of Electrical and Electronics Engineers (IEEE).
[92] Kuru, K., 2025, January. 6g in developing high-fidelity immersive digital twins. In *2nd International Conference on Communication, Information and Digital Technologies*.
[93] Kuru, K., 2025. 6G Vision in Developing Swarms of Collaborative Robotics.
[94] Kuru, K., 2024. Human-in-the-Loop Telemanipulation Modes for Autonomous Unmanned Aerial Systems.
[95] Kuru, K., (2025) *Fully Autonomous Robotic Applications Enabled by Distributed Artificial Intelligence and Fine-Tuned Large Language Models.* In: International Connect on Robotics, Autonomous & Artificial Intelligence (ROBOTCONNECT2026), March 23–24, 2026, Barcelona, Spain.
[96] Kuru, K., 2025. Collaborative Intelligence of Robotic Swarms in State and Situation Awareness and Human-Swarm Co-Work.
[97] Chkirbene, Z. *et al*.. 2025, IRS-Enhanced UAV Communication Networks: Securing Data With Hybrid Genetic and Gradient Descent Algorithms. In *2025 IEEE Wireless Communications and Networking Conference (WCNC)* (pp. 1-6). IEEE.